Journal of Applied Physics

Polarization effects in laser-induced plasma lasers based on elements from the 13th group

Cite as: J. Appl. Phys. **129**, 013103 (2021); https://doi.org/10.1063/5.0031063
Submitted: 28 September 2020 . Accepted: 16 December 2020 . Published Online: 06 January 2021

L. Nagli, E. Stambulchik, M. Gaft, and Y. Raichlin

View Online Export Citation CrossMark

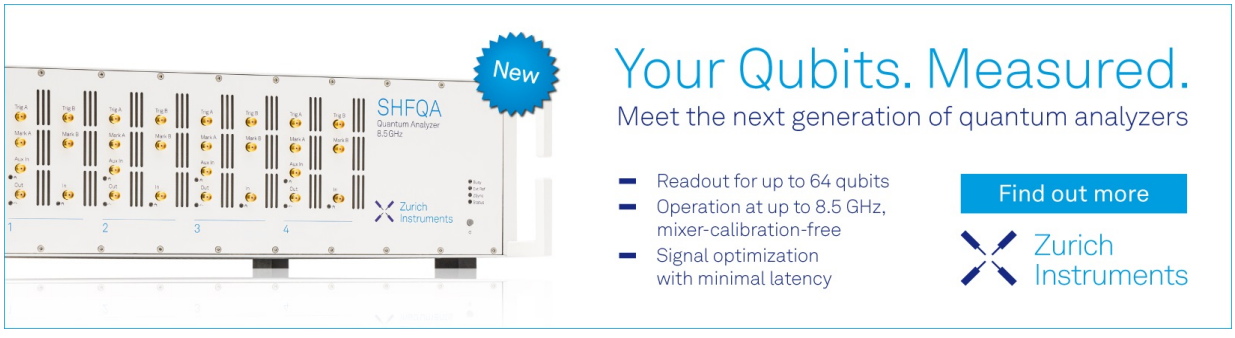

© 2021 Author(s).

Journal of Applied Physics ARTICLE scitation.org/journal/jap

Polarization effects in laser-induced plasma lasers based on elements from the 13th group

Cite as: J. Appl. Phys. **129**, 013103 (2021); doi: 10.1063/5.0031063
Submitted: 28 September 2020 · Accepted: 16 December 2020 ·
Published Online: 6 January 2021

View Online Export Citation CrossMark

L. Nagli,[1,a)] E. Stambulchik,[2] M. Gaft,[1] and Y. Raichlin[1]

AFFILIATIONS

[1]Department of Physics, Ariel University, Ariel 40700, Israel
[2]Faculty of Physics, Weizmann Institute of Science, Rehovot 7610001, Israel

[a)]**Author to whom correspondence should be addressed:** levna@ariel.ac.il

ABSTRACT

We propose a model explaining polarization effects in laser-induced plasma lasers (LIPLs) of the 13th group elements, pumped by a linearly polarized laser beam. The model is based on considering optical transitions between magnetic sublevels involved in the pumping–generation cycle. The model reproduces experimentally observed LIPL polarization features under the $np\ ^2P_{1/2,\ 3/2} \rightarrow n's\ ^2S_{1/2}$ pumping. On the other hand, polarization-resolved collisional-radiative modeling appears to be required for a quantitative explanation of the LIPL polarization when the $np\ ^2P_{1/2,\ 3/2} \rightarrow n'd\ ^2D_{1/2}$ pumping is used.

Published under license by AIP Publishing. https://doi.org/10.1063/5.0031063

I. INTRODUCTION

The lasing effect was demonstrated in laser-induced plasmas (LIPs) of elements from the 13th and 14th groups as well as Ca, Ti, Zr, Fe, Cu, Ni, and V plasmas.[1–3] The unique generation mechanism of LIP lasers (LIPLs) allows one to study a variety of LIP properties and fundamental laser plasma physics problems.

LIPLs based on elements from the 13th group having small spin–orbit splitting of the ground term (Al, Ga, In) under resonant pumping from the ground-term levels ($np\ ^2P_{1/2}$ and $np\ ^2P_{3/2}$), lase according to the three-level scheme (transitions $ns\ ^2S_{1/2} \rightarrow n'p\ ^2P_{1/2}$ or $ns\ ^2S_{1/2} \rightarrow n'p\ ^2P_{3/2}$.[1–6] Thallium (Tl), the heaviest element of this group, possesses a large spin–orbit ground-term splitting (about 1 eV) and generates differently from other 13th group elements.[2] The generation scheme for Al LIPL is presented in Fig. 1. The scheme does not include infrared direct generation from $5s\ ^2S_{1/2}$ to combined $3s^2\ 4p\ ^2P_{1/2;3/2}$ and $3s^2\ 3d\ ^2D_{3/2;5/2}$ levels.[6] The inverse population of the upper lasing levels is created through a cascade of collisional and radiative processes from higher excited states (the curved dashed lines).[4,5] It was also shown that pumping from $np\ ^2P_{1/2}$ leads to unpolarized radiation while pumping from $np\ ^2P_{3/2}$ leads to a strongly polarized generation with a degree of polarization (DOP) and the polarization direction dependent on the pumping transitions.[7] For example, in Al LIPL (Fig. 1), pumping $3p\ ^2P_{3/2} \rightarrow 5s\ ^2S_{1/2}$ (266.039 nm) leads to generation at 396.15 nm with DOP ≈ 1 and the polarization vector $\boldsymbol{E_g}$ parallel to the pumping light polarization $\boldsymbol{E_p}$, while pumping to $3d\ ^2D_{3/2;5/2}$ (309.28 nm) leads to the same generation wavelength but with $\boldsymbol{E_g} \perp \boldsymbol{E_p}$ and DOP ≈ -0.7.[7] A similar effect of polarization conservation in collisional processes was found in the generation of the optically pumped alkali atoms lasers.[8–11] The Tl LIPL generation is not polarized at all.[2]

The effects of LIPL polarization were studied in the absence of an external magnetic field and were also manifested in polarized stimulated emission (SE) in the absence of an optical resonator.[1–3]

A previous study[7] proposed that the observed polarization effects were caused by self-generated electric and magnetic fields, which break the magnetic sub-level degeneracy.[11–15] Here, we present a different model, based on fewer assumptions, explaining the polarization that considers magnetic sublevels m in the pumping–generation cycle.

II. EXPERIMENTAL SETUP

The experimental setup is similar to that described elsewhere[1,2,7] and is schematically shown in Fig. 2. In brief, a transverse pumping scheme is used.

$5 \times 20 \times 2\ mm^3$ metallic aluminum (Al), indium (In), gallium (Ga), and thallium (Tl) as TlBr crystal (KRS-5)) samples were placed inside flat–flat optical resonator. The Al coated mirrors are used. The rear mirror has a 99.9% reflection, and the output mirror has about 10% reflection. The resonator was optimized for

Published under license by AIP Publishing.

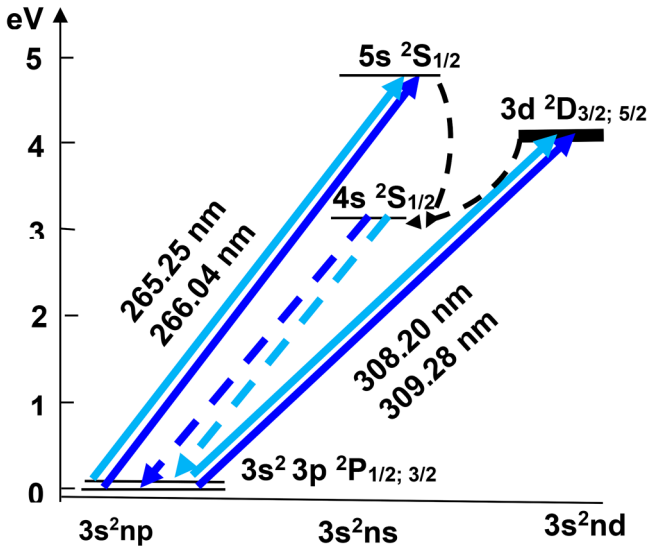

FIG. 1. A simplified scheme of the Al LIPL pumped at 265.30 nm, 266.04 nm, 308.20 nm, and 309.28 nm. The navy blue and blue arrows indicate pumping from the ground-term $3p\ ^2P_{1/2}$ and $3p\ ^2P_{3/2}$ levels, respectively (the spin–orbit splitting 0.014 eV). The black dashed arrows designate collisional transitions, leading to a population of the $4s\ ^2S_{1/2}$ level, from which a lasing occurs to the $3p\ ^2P_{1/2}$ or $3p\ ^2P_{3/2}$ levels (the dashed navy blue and blue arrows, respectively).

maximal lasing output. Nd:YAG 1.06 μm laser (LQ215-D, (pulse duration about 7 ns, pulse energy from 40 to 90 mJ/pulse) produces a plasma strip of about 5 mm in length and 0.5 mm diameter (irradiance from 1.5 to 3 J/cm^2) on a sample surface through a cylindrical lens. After a delay of 5–10 μs, (depending on the sample used), the plasma plume is pumped by an optical parametric oscillator (OPO) (RADIANT 355 LD-UV, 5 ns duration, the spectral linewidth is about 5 cm^{-1}, irradiance on plasma plume of about 0.1 J/cm^2 at resonant wavelengths of the plasma species. The plasma electron temperature T_e and electron density n_e reach about 5000 K and 10^{16} cm^{-3}, respectively, at this time.[2,3] Unlike the previous experiments, the plasma radiation is transmitted to the

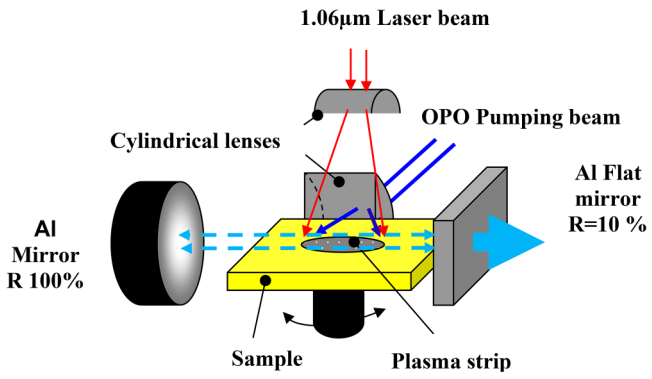

FIG. 2. Experimental setup.

Shamrock SR 750-A spectrometer (grating 2400 l/mm), equipped with a fast ICCD camera (Andor DH320-18U-03) through a custom fiber bundle (round (SMA) to the ferrule (sleet) with a 500 μm core and 1 m length). It was checked that the fiber also works as a polarization scrambler to eliminate spectrometer-induced polarization effects. The spectral and time resolution is about 0.01 nm and 1.5 ns, respectively. The line polarization is measured using the Thorlabs GL-10 calcite polarizer, placed before the optical fiber entrance. The DOP is defined as $DOP = (I_{II} - I_\perp)/(I_{II} + I_\perp)$, where I_{II} and $I_\perp$ are the generation line intensities with $\boldsymbol{E_g}$ parallel and perpendicular to $\boldsymbol{E_p}$, respectively. A λ/2 plate alters the direction of the pumping polarization vector. The geometry of the polarization measurements is shown in Fig. 3. There, $\boldsymbol{k_p}$ and $\boldsymbol{k_g}$ are the pumping, and LIPL beams wave vectors, respectively, $\boldsymbol{E_p}$ and $\boldsymbol{E_g}$ are the pumping and generation polarization vectors. The yellow cylinder is the plasma plume above a sample surface.

III. RESULTS AND DISCUSSION

As mentioned above, the upper lasing levels' population inversion is formed by collisional and radiative processes from the pumped levels.[4,5] For Al LIPL, e.g., these levels may be $5s\ ^2S$, $3d\ ^2D$, or $4\,s\ ^2S$ (see Fig. 1). On the other hand, the plasma density is too low for efficient mixing of the ground-term $^2P_{1/2}$ and $^2P_{3/2}$ levels (see also Ref. 15). Therefore, it is evident that a resonant pumping from the $^2P_{1/2}$ level will leave $^2P_{3/2}$ strongly populated, and vice versa. Accordingly, the lasing can occur only for transitions to the same level from which one pumps as indeed, it has been experimentally observed.[1–7]

The following discussion is for Al LIPL; however, the same considerations apply to the other 13th group elements as well. Tl needs some additional considerations and will be discussed in Sec. III C.

It was found that any resonant pumping from the ground level $3p\ ^2P_{1/2}$ leads to generation at 394.40 nm, which is not polarized (DOP = 0), while pumping from the $3p\ ^2P_{3/2}$ level leads to generation at 396.15 nm, the DOP of which depends on the pumping transition and its polarization direction.[7] Figure 4 presents examples of the Al LIPL generation line spectra, measured under pumping at 266.04 nm (a) and 309.28 nm (b). In both cases, black lines are the generation with $\boldsymbol{E_g}$ parallel to the $\boldsymbol{E_p}$, and red lines are the generation with $\boldsymbol{E_g}$ normal to the $\boldsymbol{E_p}$.

Table I lists measured DOP of Al LIPL for parallel (DOP_{II}) and normal ($DOP_\perp$) direction of the pumping light polarization vector $\boldsymbol{E_p}$, relatively to the lasing direction $\boldsymbol{k_g}$. Line notations are taken from Refs. 16 and 17.

The polarization effects can be explained, considering magnetic sub-levels and assuming they practically do not mix due to collisions with the plasma electrons during the pumping -generation cycle.

From now on, we assume the quantization axis to lie along with the polarization of the pumping laser $\boldsymbol{E_p}$ (Fig. 3). Figure 5 shows Al energy levels, including the magnetic sub-levels (it must be emphasized that there is no actual Zeeman splitting; the magnetic sub-levels are shown separately for the sake of clarity. The π and σ polarizations are due to transitions with $\Delta M = 0$ and $\Delta M = \pm 1$, respectively. Here, M is the projection of the total angular momentum J.

Published under license by AIP Publishing.

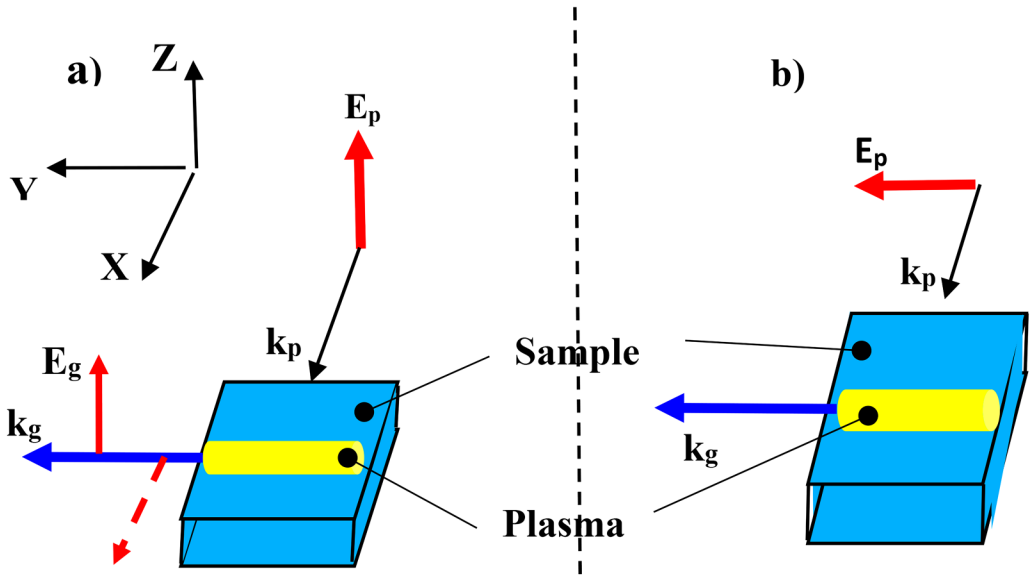

FIG. 3. The polarization measurements' geometry with the pumping beam polarization vector E_p normal (a) and parallel (b) to lasing direction vector k_g. The yellow cylinder is the plasma plume.

A. Pumping polarization vector E_p normal to the lasing direction k_g

Let us start with pumping from $^2P_{1/2}$ [see Fig. 5(a)], which is the simplest case to consider [experiments geometry is shown in [Fig 3(a)]. Indeed, the entire $^2P_{1/2}$ will be depleted, through the $^2P_{1/2;\ -1/2} \rightarrow {}^2S_{1/2;\ -1/2}$ or $^2P_{1/2;1/2} \rightarrow {}^2D_{*/2;1/2}$ (for brevity, not shown in the figure), and similarly for the negative M's: $^2P_{1/2;\ -1/2} \rightarrow {}^2S_{1/2,\ -1/2}$, etc. ($\Delta M = 0$ transitions). Hence, $^2P_{1/2,\ +1/2}$, and $^2P_{1/2,\ -1/2}$ are equally depleted, i.e., there is no preferred directionality in the system, and the lasing may occur with any polarization (DOP = 0). In other words, there should be no polarization. It is exactly what is observed in the experiments (see Table I).

We now consider pumping from $np\ ^2P_{3/2}$ to $n'\ s\ ^2S_{1/2}$ with lasing from $n''\ s\ ^2S_{1/2}$ to $np\ ^2P_{3/2}$ [Fig. 5(b)]. In this case, $^2P_{3/2;\ \pm1/2}$

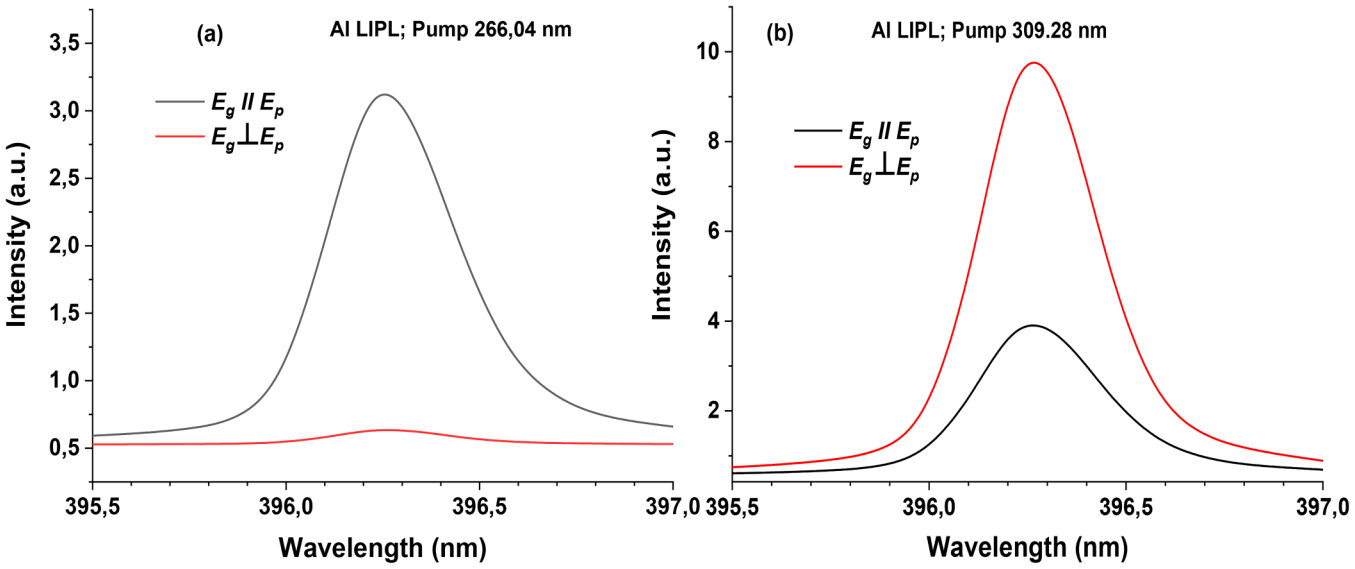

FIG. 4. Example of the Al LIPL generation line: (a) pumping 266.04 nm and (b) pumping 309.28 nm. Red curves E_g are normal to E_p, and black curves E_g are parallel to E_p.

Published under license by AIP Publishing.

TABLE I. Polarization of the Al I LIPL for the pumping polarization vector $\boldsymbol{E_p}$ normal ($DOP_\perp$) or parallel (DOP_{II}) to the lasing vector $\boldsymbol{k_g}$. $^2D_{*/2}$ means closely spaced $^2D_{3/2}$ and $^2D_{5/2}$ levels.

		Polarization	
Pumping transition, wavelength (nm)	Lasing transition, wavelength (nm)	$DOP_\perp$	DOP_{II}
$3p\ ^2P3_{1/2} \rightarrow 6s\ ^2S_{1/2}$ 237.84	$4s\ ^2S_{1/2} \rightarrow 3p\ ^2P_{3/2}$ 396.15	0.8	No generation
$3p\ ^2P_{1/2} \rightarrow 4d\ ^2D^*_{/2}$ 256.8	$4s\ ^2S_{1/2} \rightarrow 3p\ ^2P_{1/2}$ 394.4	0	0.0
$3p\ ^2P_{1/2} \rightarrow 4d\ ^2D^*_{/2}$ 257.51	$4s\ ^2S_{1/2} \rightarrow 3p\ ^2P_{1/2}$ 396.15	−0.6	0.0
$3p\ ^2P_{1/2} \rightarrow 5s\ ^2S_{1/2}$ 265.25	$4s\ ^2S_{1/2} \rightarrow 3p\ ^2P_{1/2}$ 394.40	0.0	0.0
$3p\ ^2P_{1/2} \rightarrow 3d\ ^2D_{*/2}$ 308.21	$4s\ ^2S_{1/2} \rightarrow 3p\ ^2P_{1/2}$ 394.40	0.0	0.0
$3p\ ^2P_{3/2} \rightarrow 5s\ ^2S_{1/2}$ 266.04	$4s\ ^2S_{1/2} \rightarrow 3p\ ^2P_{3/2}$ 396.15	1.0	No generation
$3p\ ^2P_{3/2} \rightarrow 3d\ ^2D^*_{/2}$ 309.28	$4s\ ^2S_{1/2} \rightarrow 3p\ ^2P_{3/2}$ 396.15	−0.7	0.0

become depleted through the $np\ ^2P_{3/2;\ \pm1/2} \rightarrow n'\ s\ ^2S_{1/2,\ \pm1/2}$ pumping, while $np\ ^2P_{3/2,\ \pm3/2}$ remain populated. In principle, there could be lasing with the linear polarization ($^2S_{1/2,\ \pm1/2} \rightarrow 3p^2P_{3/2;\ \pm1/2}$ $\Delta M = 0$) and the circular ones ($^2S_{1/2,\ \pm1/2} \rightarrow {}^2P_{3/2,\ \mp1/2}$, $\Delta M = \pm 1$). However, each circularly polarized photon would be absorbed through the $^2P_{3/2,\ \pm3/2} \rightarrow {}^2S_{1/2,\ \pm1/2}$ processes. Thus, only the linearly polarized ($\Delta M = 0$) photons survive and lase. The polarization degree is indeed close to unity in the corresponding experiments (see Table I).

Finally, let us discuss the scheme with pumping $^2P_{3/2}$ to $^2D_{3/2,5/2}$ (hereafter $^2D_{*/2}$) with the lasing occurring from $^2S_{1/2}$ to $\rightarrow {}^2P_{3/2}$; it is the most complicated case.

At first glance, it appears that there should be no polarization at all since all $^2P_{3/2}$ projections should be depleted through $^2P_{3/2,\ \pm1/2} \rightarrow {}^2D_{*/2,\ \pm1/2}$ and $^2P_{3/2,\ \pm3/2} \rightarrow {}^2D_{*/2,\ \pm3/2}$. However, we need to consider the "next order" corrections, namely, excitations and de-excitations due to the plasma electrons (which, besides, might be preferably oscillating in one direction due to the laser field present, further breaking the symmetry).[18] This effect is well known in x-ray lasers.[19–21] A detailed polarization-resolved collisional-radiative (CR) model is likely required to explain the observations in this case.

CR model should account for multiple levels of the neutral and at least singly ionized charge state of the atom, with all levels resolved to their magnetic sub-levels in order to account for polarization effects to be inferred. The atomic processes accounted for must include electron impact excitation and de-excitation, electron impact ionization and recombination, radiative recombination, and radiative decay (including stimulated one in the presence of the pumping laser field and later, the LIPL radiation). Also, collisions with the heavy particles (neutral atoms and ions) are likely very important in relaxation of the atomic state alignment by mixing magnetic sub-levels belonging to the same level.[22] Furthermore, the motion of the free plasma electrons in the laser field's presence acquires a directionality, which in turn introduces alignment effects in the atomic level populations on its own. Building such a comprehensive computational model is a formidable task, which is beyond the scope of the present study. There are no existing general-purpose CR codes with all the features listed above implemented to

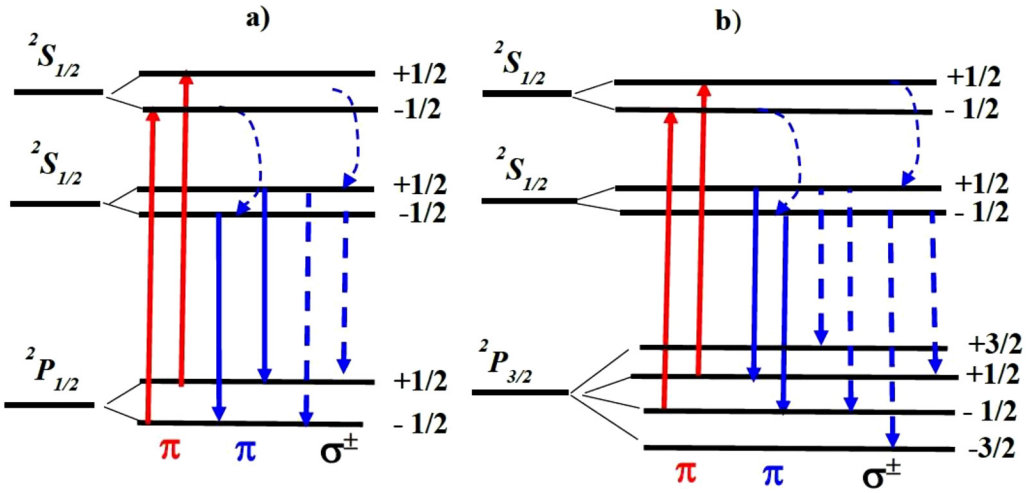

FIG. 5. Energy schemes for pumping from $^2P_{1/2}$ (a) and $^2P_{3/2}$ (b), including the magnetic sublevels. The red lines are the (π-polarized) pumping, and the blue solid and dashed arrows are the π and $\sigma^\pm$ circularly polarized generation, respectively. The blue dashed curves are the collisional processes.

Published under license by AIP Publishing.

TABLE II. Polarization of In LIPL when pumping polarization vector $\boldsymbol{E_p}$ is normal (DOP$_\perp$) to the lasing direction vector $\boldsymbol{k_g}$ direction.

Pumping		Lasing		
Transition	Wavelength (nm)	Transition	Wavelength (nm)	Polarization DOP$_\perp$
$5p\ ^2P_{1/2} \rightarrow 8s\ ^2S_{1/2}$	246.01	$6s\ ^2S_{1/2} \rightarrow 5p\ ^2P_{1/2}$	410.17	0.0
$5p\ ^2P_{1/2} \rightarrow 6d\ ^2D_{3/2}$	256.01	$6s\ ^2S_{1/2} \rightarrow 5p\ ^2P_{1/2}$	410.17	0.0
$5p\ ^2P_{1/2} \rightarrow 7s\ ^2S_{1/2}$	275.39	$6s\ ^2S_{1/2} \rightarrow 5p\ ^2P_{1/2}$	410.17	0.0
$5p\ ^2P_{1/2} \rightarrow 5d\ ^2D_{3/2}$	303.93	$6s\ ^2S_{1/2} \rightarrow 5p\ ^2P_{1/2}$	410.17	0.0
$5p\ ^2P_{3/2} \rightarrow 8s\ ^2S_{1/2}$	260.17	$6s\ ^2S_{1/2} \rightarrow 5p\ ^2P_{3/2}$	451.3	1.0
$5p\ ^2P_{3/2} \rightarrow 6d\ ^2D_{3/2}$	271.39	$6s\ ^2S_{1/2} \rightarrow 5p\ ^2P_{3/2}$	451.3	−0.9
$5p\ ^2P_{3/2} \rightarrow 6d\ ^2D_{5/2}$	271.03	$6s\ ^2S_{1/2} \rightarrow 5p\ ^2P_{3/2}$	451.3	0.75
$5p\ ^2P_{3/2} \rightarrow 7s\ ^2S_{1/2}$	293.26	$6s\ ^2S_{1/2} \rightarrow 5p\ ^2P_{3/2}$	451.3	1.0
$5p\ ^2P_{3/2} \rightarrow 5d\ ^2D_{3/2}$	325.86	$6s\ ^2S_{1/2} \rightarrow 5p\ ^2P_{3/2}$	451.3	−0.85
$5p\ ^2P_{3/2} \rightarrow 5d\ ^2D_{5/2}$	325.61	$6s\ ^2S_{1/2} \rightarrow 5p\ ^2P_{3/2}$	451.3	−0.65

the best of our knowledge. We hope the experimental results presented in this study will serve as an incentive to implement such a model, which will certainly be important for analyzing radiation's polarization properties in the course of laser–matter interactions in a broad context.

B. Pumping polarization parallel to the lasing direction

It has been found that in this geometry [see Fig. 3(b)], similar to the normal pumping discussed above, pumping from the $3p\ ^2P_{1/2}$ level leads to an unpolarized generation at 394.40 nm. However, when pumping 266.04 nm ($3p\ ^2P_{3/2} \rightarrow 5\,s\ ^2S_{1/2}$), the lasing entirely disappears, while pumping at 309.28 nm ($3p\ ^2P_{3/2} \rightarrow 3d\ ^2D_{\star/2}$,) the generated light is unpolarized.

In the case of pumping from $^2P_{1/2}$, the same as in Sec. III A, considerations apply, with no polarization expected.

For pumping from $^2P_{3/2}$ to $^2S_{1/2}$ and lasing from $^2S_{1/2}$ to $^2P_{3/2}$, we again repeat the same arguments as in Sec. III A. However, the quantization axis is now the same as the laser beam propagation direction. Since a photon may have only $M = \pm 1$ projection in its direction, it immediately follows that there should be no lasing at all. In fact, for the very same reason, it can be concluded that for any combination of the pumping and lasing transitions, only $\Delta M = \pm 1$ transition would emit photons propagating along the line of sight in this (pumping parallel to the lasing direction) configuration. If everything is perfectly aligned, there should be no difference between $\Delta M = +1$ and $\Delta M = -1$, and thus, the lasing should be unpolarized when allowed at all. Indeed, this is observed in our experiments. This concludes the discussion of Table I.

C. Other species from the 13th group

It must be emphasized that all considerations above are valid only for small spin–orbital splitting Δ_{LS} of the ground np levels ($n = 3$, 4, and 5 for Al, Ga, and In, respectively), such that $\Delta_{LS} \ll T_e$ under our experimental conditions. For these elements, the ground-term $^2P_{1/2;\ 3/2}$ levels are about equally populated, which prevents the $\sigma^{\pm}$ generation in $n's\ ^2S_{1/2} \rightarrow np^2P_{3/2}$ transitions under linearly polarized pumping. Table II lists measured DOP$_\perp$ of In LIPL for the pumping light polarization vector $\boldsymbol{E_p}$ normal to $\boldsymbol{k_g}$.

We note that the lasing polarization properties are retained even when pumped to higher $^2S_{1/2}$ or $^2D_{\star/2}$ states (see Tables I and II). Apparently, during the longer times required for forming the inversion population through a cascade of collisional-radiative processes in this case, the ground-term levels remain aligned.

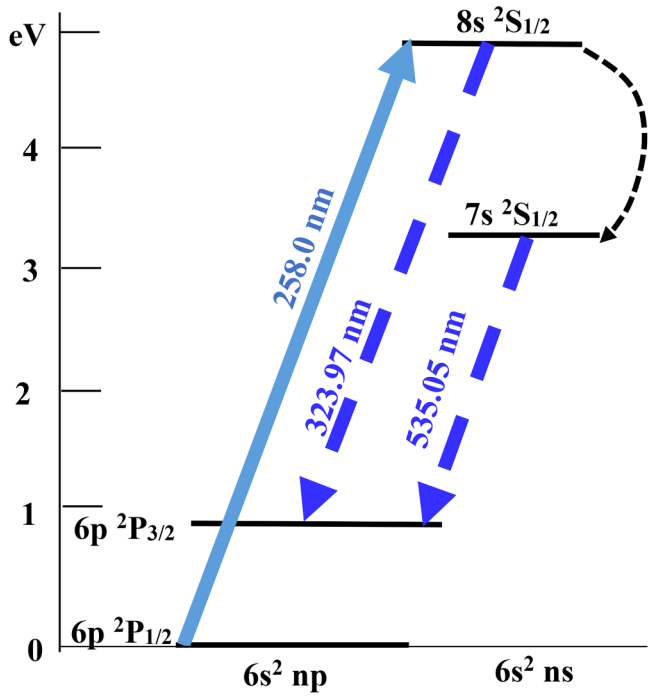

FIG. 6. A simplified scheme of the lasing levels of Tl LIPL pumped at 258 nm. The solid arrow is the pumping transition starting from the ground $6s^2\ 3p\ ^2P_{1/2}$ level. The curved dashed arrows are collisional transitions. The dashed blue arrows are the generation to the $3p\ ^2P_{1/2}$ and $3p\ ^2P_{3/2}$ ground levels.

Published under license by AIP Publishing.

In the case of In LIPL, we were able to pump $5p\ ^2P_{3/2} \rightarrow 6d\ ^2D_{3/2}$, and $^2D_{5/2}$ separately. It is found that in In LIPL under the $5p\ ^2P_{3/2} \rightarrow 6d\ ^2D_{*/2}$ pumping, the DOP sign changes from (−) to (+). It needs additional theoretical considerations on the base of the CR model.

However, in the Tl atom case, the ground configuration splitting is significant ($\Delta_{LS} = 0.98$ eV, see Fig. 6), and, therefore, the $6p\ ^2P_{3/2}$ states are populated very weakly. Consequently, pumping $6p\ ^2P_{1/2} \rightarrow 8s\ ^2S_{1/2}$ (258.00 nm) leads to direct generation $8s\ ^2S_{1/2} \rightarrow 6p\ ^2P_{1/2}$ (323.97 nm), and $7s\ ^2S_{1/2} \rightarrow 6p\ ^2P_{3/2}$ (535.05 nm); this is a four-level lasing scheme. By repeating arguments in Sec. III A, all magnetic sublevels of $6p\ ^2P_{3/2}$ are equally depopulated, and the reabsorption of the $\sigma^{\pm}$ photons, contrary to the Al LIPL, is absent. Therefore, according to the proposed model, both generations should not have been polarized, and it is experimentally confirmed.

IV. CONCLUSIONS

We studied polarization properties of the 13th group (Al, Ga, In, and Tl) LIPLs, pumped by resonant, linearly polarized light pulses in the absence of the external magnetic field. Measurements were done in the transverse pumping geometry with the pumping beam polarization $\boldsymbol{E_p}$ normal or parallel to generation direction $\boldsymbol{k_g}$. For atoms with the spin–orbit splitting $\Delta_{LS} \ll T_e$ (Al, Ga, In) generation occurs according to the three-level generation scheme. The polarization effects were explained, considering magnetic sub-levels and assuming that they practically do not mix due to collisions with the plasma electrons during the pumping–generation cycle. The absence of the polarization in the generation $n's\ ^2S_{1/2,\pm1/2} \rightarrow np\ ^2P_{1/2,\pm1/2}$ under the pumping $np\ ^2P_{1/2,\pm1/2} \rightarrow n''\ s\ ^2S_{1/2,\pm1/2}$ is explained by equal depletion of the magnetic sublevels of $np\ ^2P_{1/2}$ by the linearly polarized pumping light and equally probable transitions to these sublevels, giving π and $\sigma^{\pm}$ generation and as a result nonpolarized generation. Accordingly, pumping $np\ ^2P_{3/2,\ \pm1/2\ \pm3/2} \rightarrow n's\ ^2S_{1/2,\ \pm1/2/}$ leaves the $2P_{3/2,\ \pm3/2}$ states fully populated, preventing the $\sigma^{\pm}$ transitions ($^2S_{1/2,\ \pm1/2} \rightarrow {}^2P_{3/2,\mp1/2}$, $\Delta M = \Delta M = \pm 1$) due to the self-absorption. As a result, only π polarization transitions ($^2S_{1/2,\ \pm1/2} \rightarrow 3p^2P_{3/2,\ \pm1/2}\ \Delta M = 0$) lase. The absence of polarization in the Tl LIPL generation, predicted by these considerations, confirms the proposed model in the Al, Ga, and In LIPL. Polarization properties of the 13th group elements pumped to the $^2D_{*/2}$ states need additional theoretical consideration, likely requiring a polarization-resolved collisional-radiative model.

DATA AVAILABILITY

The data that support the findings of this study are available within the article and its supplementary material.

REFERENCES

[1]L. Nagli and M. Gaft, Opt. Commun. **354**, 330 (2015).
[2]L. Nagli1, M. Gaft, I. Gornushkin, and R. Glaus, Opt. Commun. **378**, 41 (2016).
[3]R. Glaus, I. Gornushkin1, and L. Nagli, Appl. Opt. **56**, 3699 (2017).
[4]I. Gornushkin, R. Glaus, and L. Nagli, Appl. Opt. **56**, 695 (2017).
[5]I. B. Gornushkin and A. Y. Kazakov, J. Appl. Phys. **121**, 213303 (2017).
[6]L. Nagli1, M. Gaft, Y. Raichlin, and I. Gornushkin, Opt. Commun. **415**, 127 (2018).
[7]L. Nagli1 and Y. Raichlin, Opt. Commun. **447**, 51 (2019).
[8]A. Mironov and J. Eden, in Frontiers in Optics/Laser Science 2016, paper JTh2A.12.
[9]A. E. Mironov and J. G. Eden, Opt. Express **25**, 29676 (2017).
[10]A. E. Mironov, J. D. Hewitt, and J. G. Eden, Phys. Rev. Lett. **118**, 113201 (2017).
[11]H. M. Milchberg and J. C. Weisheit, Phys. Rev. A **26**, 1023 (1982).
[12]A. K. Sharma and R. K. Thareja, J. Appl. Phys. **98**, 033304 (2005).
[13]A. K. Sharma and R. K. Thareja, Appl. Surf. Sci. **253**, 3113 (2007).
[14]G. A. Wubetu, H. Fiedorowicz, J. T. Costello, and T. J. Kelly, Phys. Plasmas **24**, 013105 (2017).
[15]N. Fortson and B. Meckel, Phys. Rev. Lett. **59**, 1281 (1987).
[16]See http://physics.nist.gov/PhysRefData/ASD/lines_form.html for NIST, Atomic Spectra Database Lines.
[17]P. Smith, C. Heise, J. Esmond, and R. Kurucz, see http://www.pmp.uni-hannover.de/cgi-bin/ssi/test/kurucz/sekur.html.
[18]Y. Zel'dovich and Y. Raizer, *Physics of Shock Waves and High-Temperature Hydrodynamic* (Phenomena, Dover Publications, Mineola, NY, 2002), pp. 382–421.
[19]B. Rus, C. L. S. Lewis, G. F. Cairns, P. Dhez, P. Jaegle, M. H. Key, D. Neely, A. G. MacPhee, S. A. Ramsden, C. G. Smith, and A. Sureau, Phys. Rev. A **51**, 2316–2327 (1995).
[20]U. Fano and J. H. Macek, Rev. Modern Phys. **45**, 553 (1973).
[21]K. Janulewicz, C. Kim, H. Stie, T. Kawachi, M. Nishikino, and N. Hasegawa, Proc. SPIE **9589**, 958901 (2015).
[22]S. Kazantsev and J. Hénoux, *Polarization Spectroscopy of Ionized Gases* (Springer-Science + Business Media, B.V, 1995).

Published under license by AIP Publishing.